

# Interaction of light with a single atom in the strong focusing regime

Syed Abdullah Aljunid<sup>1</sup>, Brenda Chng<sup>1</sup>, Martin Paesold<sup>1,2</sup>, Gleb Maslennikov<sup>1</sup> and Christian Kurtsiefer<sup>1\*</sup>

<sup>1</sup>Centre for Quantum Technologies / Department of Physics, National University of Singapore, Singapore and

<sup>2</sup>ETH Zürich, Switzerland

(Dated: March 21, 2022)

We consider the near-resonant interaction between a single atom and a focused light mode, where a single atom localized at the focus of a lens can scatter a significant fraction of light. Complementary to previous experiments on extinction and phase shift effects of a single atom, we report here on the measurement of coherently backscattered light. The strength of the observed effect suggests combining strong focusing with the well-established methods of cavity QED. We consider theoretically a nearly concentric cavity, which should allow for a strongly focused optical mode. Simple estimates show that in a such case one can expect a significant single photon Rabi frequency. This opens new perspectives and a possibility to scale up the system consisting of many atom+cavity nodes for quantum networking due to a significant technical simplification of the atom–light interfaces.

## I. INTRODUCTION

In order to manage more complex tasks in quantum communication and information processing, it became obvious in the recent years that different physical systems have different strengths in various quantum information processing primitives. Thus, different quantum systems have to be combined for more complex tasks, and interfaces between various microscopic systems and photons in the optical domain — as quantum information carriers which allow easy decoherence-free transport of quantum information — are of strong interest.

To accomplish a substantial information exchange between photons and microscopic systems like atoms, or to implement an atom-mediated interaction between flying qubits, a strong interaction between the photons and atoms is essential. So far, the canonical approach to this problem in the makes use of cavities with a high finesse and a small mode volume. This significantly enhances the electrical field of a single photon such that the atomic state could be substantially affected [1]. This technique has been proven to be amazingly successful [2–5], but it remains a technological challenge to work with such cavities. Despite the dramatic success in increasing resonator finesse with smart dielectric structures [4], the bulk of cavity QED experiments in the optical domain still makes use of cavities based on sophisticated dielectric coatings [6–8], which are still an art to make. This, together with the challenge to stabilize the cavities against vibrations make it seem hard to scale up such atom–light interfaces to the desired quantum networks [9].

An alternative approach for increasing the electromagnetic field at the location of an atom considers strong focusing of the optical mode. This technique has been applied to observe strong interaction of the electromagnetic fields with molecules [10, 11], quantum dots [12], and single atoms [13, 14] as possibly one of the cleanest physical systems for quantum information processing.

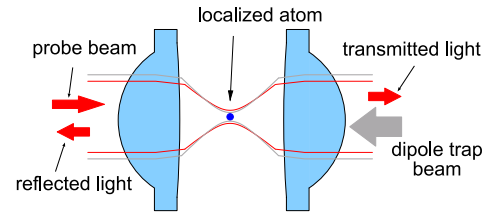


FIG. 1: Concept of an atom interacting with a Gaussian light mode using a pair of lenses.

The basic configuration of such an interaction scheme is shown in figure 1. Efforts are under way to reach near perfect coupling between field modes and electrical dipole transitions in ions [15].

In this paper, we report on measurements of the reflection of light in a tightly focused mode by a single atom in section II, complementing the observation of transmission [13] and phase shift [14]. The essence of such experiments can be understood by treating the light field classically, since the focusing geometry only modifies the boundary conditions of the electromagnetic field.

In order to investigate the interaction between light and the atom on the single photon level, however, we need to move on to a quantized description of the electromagnetic field. In section III, we describe how the effects of the boundary conditions in a strong focusing regime can be integrated into a quantized description of the electromagnetic field. We consider both running wave geometries, which connect to ‘flying qubits’, i.e., for a continuous mode spectrum of the field, and a discrete mode spectrum as it may be found in resonator configurations. The strong enhancement of the light field due to focusing may open a complementary route to bring atom–light interaction into the strong coupling regime, which for now was achievable only with the aid of small cavities with a high finesse. In section IV, we follow up on earlier ideas of cavities with a small focus [16, 17] and estimate the coupling strength in a Jaynes–Cummings model of atom–field interaction for a cavity which combines our strong focusing results with a resonator.

\*christian.kurtsiefer@gmail.com; <http://www.quantumlah.org>

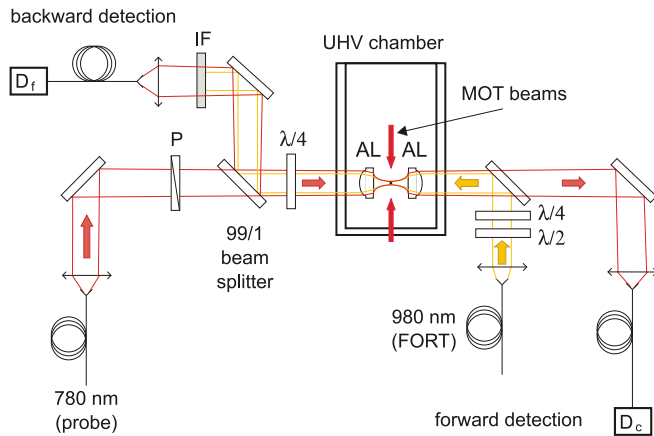


FIG. 2: Experimental setup for measuring extinction/reflection. A single atom is localized in the focus of two lenses with a far-off resonant trap, and exposed to the focused probe light field. Transmission and reflection measurements are carried out with single photon detectors behind single mode fibers in forward and backward direction.

## II. EXPERIMENTAL OBSERVATION OF BACKSCATTERING FROM A SINGLE ATOM

To complement our earlier measurements on the transmission of a light beam focused on an atom and the atom-induced phase shift, we measured the reflection of light into the source mode by the atom. Such a reflectivity has been shown to be perfect in the idealized case of an electrical field that exactly matches a directional dipole wave [18]. However, such an electric field is not easily prepared in practice, so light fields with a Gaussian envelope are commonly used instead, as they emerge in a good approximation from optical fibers. There, the maximal reflectivity for circularly polarized light is limited to about 53% [19].

A schematic outline of our experiment is shown in figure 2. A single  $^{87}\text{Rb}$  atom is localized at the focus of two aspheric lenses with a circularly polarized far-off resonant dipole trap (FORT) with an operating wavelength of 980 nm in an ultrahigh vacuum chamber. Prior to localizing the atom, its kinetic energy is lowered to 15–30  $\mu\text{K}$  with the aid of a magneto-optical trap and a subsequent molasses cooling step. A probe beam emerging from a single mode optical fiber with a wavelength of  $\lambda = 780\text{ nm}$  is prepared into a circular polarization state, and sent through the same lens pair in a counter-propagating direction. Its frequency can be tuned over the transition from the  $5S_{1/2}, F = 2$  electronic ground state to the  $5P_{3/2}, F = 3$  excited state, and has a waist parameter of  $w_L = 1.25\text{ mm}$  just before the focusing lens with  $f = 4.5\text{ mm}$ . The transmitted light is collimated by an identical lens, and coupled into another single mode optical fiber, from where it reaches a photon counting module,  $D_c$ . To capture the reflected light, a 99:1 beam splitter is inserted into the probe beam prior to the lens arrangement, such that most of the reflected light can be

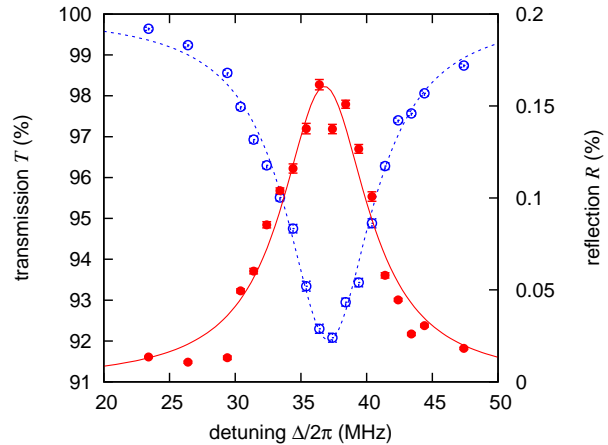


FIG. 3: Combined results for transmission and reflection from the atom–lens setup as a function of the detuning with respect to the unperturbed atomic transition. For this focusing strength, we observe a maximal reflection of 0.17% of the incoming power (open circles), coinciding with the minimal transmission of 92% (filled circles).

directed into another single mode optical fiber and detected by a second single photon detector,  $D_f$ . Dichroic mirrors and an interference filter are used to suppress the residual trap light propagating in this direction. Detector  $D_f$  is also used to observe the fluorescence from an atom in the FORT during the loading process from the magneto-optical trap. To avoid optical pumping into the  $F = 1$  ground state, re-pump light at  $\lambda = 795\text{ nm}$  resonant with the D1 line is used to transfer the atom back to the approximate two-level system via the  $5P_{1/2}, F = 2$  level. Details of the loading and state preparation sequence can be found in [13].

The results from the transmission and reflection measurement obtained by sweeping the frequency of the probe beam across the resonance are shown in figure 3. The transmission results are obtained by normalizing the events observed in detector  $D_c$  for a particular detuning in the presence of an atom to events in a time interval without the atom. Similarly, the reflectivity is obtained by normalizing the events detected with  $D_f$  against the normalization events in detector  $D_c$  without an atom in the trap. On resonance, the number of events observed in detector  $D_f$  was about  $13\text{ s}^{-1}$  above the detector background ( $100\text{--}400\text{ s}^{-1}$ ), and the data points shown were obtained by collecting events over an integration time of 50 minutes per point. Error bars depicted in the graph represent propagated Poissonian counting statistics into the final reflection/transmission value.

Both transmission and reflection measurements seem to follow the expected Lorentzian line profile. A best fit of our data to such a profile (solid lines in figure 3) with center detuning  $\Delta f_0$ , full width of half maximum (FWHM)  $\delta f$ , and amplitude as free parameters for the transmission measurement results in  $\Delta f_0 = 37.1 \pm 0.1\text{ MHz}$  and  $\delta f = 8.1 \pm 0.3\text{ MHz}$ , and a maximal extinction value of  $1 -$

$T = 8.2 \pm 0.2\%$ . For the reflection measurement, we find  $\Delta f_0 = 36.8 \pm 0.2$  MHz,  $\delta f = 8.0 \pm 0.6$  MHz, and a peak reflectivity of  $0.161 \pm 0.007\%$ .

The reflection/transmission measurements show complementary dependency on the detuning within our experimental uncertainty. The center frequency of the resonance line is shifted to the blue due to the AC Stark shift induced by the optical dipole trap, and the observed widths are slightly larger than the natural line width of the probed D2 line (6.06 MHz).

As shown in [19], the transmission and reflection properties can be derived from a dimensionless quantity

$$R_{sc}(u) = \frac{3}{4u^3} e^{2/u^2} \left[ \Gamma\left(-\frac{1}{4}, \frac{1}{u^2}\right) + u\Gamma\left(\frac{1}{4}, \frac{1}{u^2}\right) \right]^2, \quad (1)$$

which for a small focusing parameter  $u = w_L/f$  has the interpretation of a scattering probability of a photon from the atom, and exhibits a maximum of about 1.4 for  $u \approx 2$ . The focusing parameter itself is connected to the Gaussian beam divergence  $\Theta$  via  $\tan \Theta = u$ . For collection into modes overlapping with the excitation mode, the extinction  $1 - T$  and reflectivity  $R$  are given by

$$1 - T = 1 - \left| 1 - \frac{R_{sc}}{2} \right|^2 \quad \text{and} \quad R = R_{sc}^2/4. \quad (2)$$

The amplitude coefficient of the fit to the transmission measurement for this model corresponds to  $R_{sc} = 0.083 \pm 0.002$ , and the reflectivity result to  $R_{sc} = 0.080 \pm 0.002$ . Both values are in agreement within experimental uncertainties. In our experiment, however, we used a focusing parameter  $u = 0.278$  corresponding to  $R_{sc} = 0.201$ . Apart from lens imperfections, a very likely explanation for this discrepancy is the delocalization of the atom from the focus due to its residual kinetic energy, which would reduce both the electrical field felt by the atom as well as the overlap of the radiated field with the receiving modes. A quantitative numerical estimation of this effect is in preparation [20].

From this experiment, it seems that the transmission and reflection properties for light in a strongly focused mode are well understood, and motivates further investigation of atom–light interaction in the strong focusing regime.

### III. FIELD QUANTIZATION FOR FOCUSED GAUSSIAN MODES

The field quantization of Gaussian beams is relatively straightforward and has been done many times in the paraxial regime [21]. We quickly revisit one approach here, mostly to clarify the nomenclature we use later on for the strongly focused scenario. For simplicity, we begin with periodic boundary conditions and a ‘quantization length’  $L$ .

We start with an expression for the electric field operator in a generalized mode decomposition,

$$\hat{\mathbf{E}}(\mathbf{x}, t) = i \sum_j \mathcal{E}_{\omega_j} \left[ \mathbf{g}_j(\mathbf{x}) \hat{a}_j(t) - \mathbf{g}_j^*(\mathbf{x}) \hat{a}_j^\dagger(t) \right], \quad (3)$$

where the spatial dependency and polarization property of a mode  $j$  is covered by a mode function  $\mathbf{g}_j(\mathbf{x})$  and the time dependency by the ladder operators  $\hat{a}_j, \hat{a}_j^\dagger$ . The dimensional components, together with a normalization of the mode function, are lumped into the constant  $\mathcal{E}_{\omega_j}$ .

The free field Hamiltonian of the total field

$$\hat{H}_0 = \frac{\epsilon_0}{2} \int d\mathbf{x} \left[ \hat{\mathbf{E}}^2(\mathbf{x}) + c^2 \hat{\mathbf{B}}^2(\mathbf{x}) \right] \quad (4)$$

then can be written as a sum of contributions from different modes  $j$ :

$$\hat{H}_0 = \sum_j \hat{H}_j = \sum_j \frac{\epsilon_0}{2} \int d\mathbf{x} \left[ \hat{\mathbf{E}}_j^2(\mathbf{x}) + c^2 \hat{\mathbf{B}}_j^2(\mathbf{x}) \right]. \quad (5)$$

For a given mode  $j$ , the mode function  $\mathbf{g}_j(\mathbf{x})$  has to be compatible with the Maxwell equations for an angular frequency of  $\omega_j$ , and the normalization constant  $\mathcal{E}_{\omega_j}$  needs to be chosen that  $\hat{H}_j$  coincides with the Hamiltonian of a harmonic oscillator. This leads to

$$\mathcal{E}_{\omega_j} = \sqrt{\frac{\hbar \omega_j}{2\epsilon_0 V_j}}, \quad (6)$$

with an effective mode volume  $V_j$  given by

$$V_j := \frac{1}{2} \int d\mathbf{x} \left[ |\mathbf{g}_j(\mathbf{x})|^2 + \frac{c^2}{\omega_j^2} |\nabla \times \mathbf{g}_j(\mathbf{x})|^2 \right]. \quad (7)$$

In vacuum, electric and magnetic contributions to the total field energy are the same, such that we can reduce the above integral to the simplified expression

$$V_j = \int d\mathbf{x} |\mathbf{g}_j(\mathbf{x})|^2. \quad (8)$$

In the following, we now restrict the treatment of the electromagnetic field to a single mode  $j$  of the electromagnetic field, and drop the mode index. In paraxial optics, a Gaussian beam is characterized by the waist  $w_0$  and the longitudinal mode index, usually described by a wave number  $k_j$ . In a regime where there is no significant wavefront curvature (i.e.,  $L$  is smaller than the Rayleigh range  $z_R = \pi w_0^2/\lambda$ ), the mode function is given by

$$\mathbf{g}(\mathbf{x}) = \boldsymbol{\epsilon} e^{-\rho^2/w_0^2} e^{ikz}, \quad (9)$$

with a radial distance  $\rho$ , a transverse polarization vector  $\boldsymbol{\epsilon}$ , and a position  $z$  along the propagation direction. The dispersion relation for this mode is given by  $\omega^2 = c_0^2(k^2 + 2/w^2)$ . The spatial integration in eq. (8) is well-defined if the volume in propagation direction  $z$  is restricted to

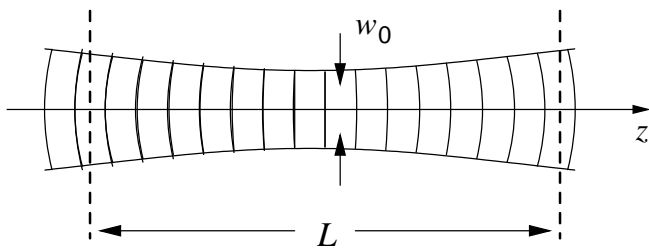


FIG. 4: Quantization geometry of a Gaussian beam of a waist  $w_0$ . To discretize the mode longitudinal mode index, we introduce periodic boundary conditions with a quantization length  $L$ .

the quantization length  $L$  (see Fig. 4), leading to a result for the effective mode volume of

$$V = \pi L w^2 / 2, \quad (10)$$

and consequently to a normalization constant  $\mathcal{E}$  of

$$\mathcal{E} = \sqrt{\frac{\hbar \omega}{\pi w^2 L \epsilon_0}}. \quad (11)$$

This expression is valid in a regime where the variation of the beam waist  $w$  along the interval in  $z$  direction does not change, i.e., the quantization length  $L \ll z_R$ . It turns out that this restriction is actually not necessary, and we can easily extend this result to focused beams.

### A. Strong focusing limit

To consider focused Gaussian beams, we keep in mind that even in a strong focusing regime ( $u$  large), light propagates either in  $+z$  or  $-z$  direction, i.e., all the optical power transported in the mode has to pass through each transverse plane. Hence, the contribution to the volume integral for each slice  $dz$  in eq. (7) is independent of  $z$ . Attention only has to be paid *where* the modulus of  $\mathbf{g}(\mathbf{x})$  is referenced to 1. For the case  $L \ll z_R$  treated above, the mode function can be chosen to  $|\mathbf{g}(\mathbf{x})| = 1$  on the entire optical axes. If one includes any focusing of the Gaussian mode,  $|\mathbf{g}(\mathbf{x})|$  varies along the optical axes, and will show a maximum in the focus. In a regime where the paraxial approximation is still valid, we can simply use the waist  $w = w_f$  in the focus in eq. (11) to obtain the correct normalization constant.

In the strong focusing regime where the paraxial approximation breaks down, a slightly different approach has to be used to estimate the electrical field at the location of the atom. Again, we start with a Gaussian mode at a location far away from the focus; for convenience, we consider a configuration as depicted in figure 1. We assign a Gaussian beam waist  $w_L$  at the collimated part of the beam outside the lens pair, and choose the mode function such that there,  $|\mathbf{g}(\mathbf{x})| = 1$  on the optical axis. The ratio of the electrical field amplitude on the axis before the lens pair,  $E_L$ , and in the focus of the system,  $E_A$ ,

can be expressed in a closed form for circularly polarized light. This ratio is determined by the numerical aperture of the focusing setup, which for Gaussian beams is better described by the focusing parameter  $u = w_L/f$ . One can show [19] that

$$\left(\frac{E_A}{E_L}\right)^2 = \frac{\pi^2 w_L^2 R_{sc}(u)}{3\lambda^2}. \quad (12)$$

We now can take the normalization expression from eq. (11) with a waist  $w_L$  before the lens, and multiply it with the field ratio determined by eq. (12) due to the focusing; we arrive at

$$\mathcal{E} = \sqrt{\frac{\pi \hbar \omega R_{sc}(u)}{3\lambda^2 L \epsilon_0}}. \quad (13)$$

The normalization constant now only depends on the wavelength, quantization length and focusing strength (or divergence) of the mode.

### B. Wave packets

To include wave packets of light in a quantized field description, a continuous mode decomposition is helpful, in which ‘localized photons’ can be expressed as a superposition of contributions from a continuous one-dimensional spectrum of modes, labeled by a continuous longitudinal wave number  $k = \omega/c$ , or the angular frequency  $\omega$  directly. Our treatment above is valid for such a case if we apply the simple transition  $L \rightarrow \infty$ , and replace the discrete sum over modes e.g. in eq. (3) by an integral:

$$\sum_j \rightarrow \frac{L}{2\pi c} \int d\omega \quad (14)$$

The expression for the normalization constants  $\mathcal{E}$  still can be taken from the expressions above, and in all physically meaningful quantities the length  $L$  should not appear anymore. Such a field decomposition allows the treatment of wave packets of various shapes. In particular, it allows to understand the dynamics of the absorption of single photon states [15, 22] or pulsed coherent states of the field.

### C. Combination with optical cavities

The introduction of a quantization length  $L$  for the field quantization has the big advantage that the mode spectrum of the electromagnetic field becomes discrete, and interaction of an atom with a single field mode can be investigated. Among other reasons, a discrete mode spectrum allows for a reasonably clean definition of what is meant by a single photon; for a continuum of modes, this is more ambiguous.

The field-enhancing effect of a small focus (‘hourglass modes’) has been identified as a method for enhancement of the electrical field in an optical cavity at the location of atoms before [16, 17]. Here, we would like to extend the description of the electrical field to strongly focused modes.

The simplest transition from the treatment presented above to a resonant structure involves a ring cavity, which reflects exactly the periodic boundary conditions above. Thus, we can directly use eq. (13) for the normalization constant  $\mathcal{E}$  for this case.

For the more conventional cavities with a standing wave field mode, quantization can be adapted from the case of periodic boundary conditions by modifying the propagating part of the mode: the  $e^{ikz}$  term has to be replaced with the standing wave component  $\sin(kz)$  for a proper choice of origin, and  $k = N\pi/L$  with an integer  $N$ . Compared to periodic boundary conditions, the  $\sin^2(kz)$  modulation in the field energy density reduces the effective mode volume by a factor of 2, and the normalization constant  $\mathcal{E}$  is given by

$$\mathcal{E} = \sqrt{\frac{2\pi\hbar\omega R_{sc}(u)}{3\lambda^2 L \epsilon_0}}. \quad (15)$$

For a standing wave resonator, the field amplitude has also a strong variation in longitudinal direction. To ensure a strong coupling of an atom with the resonator mode, the atom needs to be localized close to the anti-node of the standing wave.

#### IV. ESTIMATION OF COUPLING PARAMETERS

Since a large fraction of the scientific work on strong atom–light coupling is carried out where field modes are supported by a cavity with a discrete mode spectrum, we estimate quantitatively the combination of the field enhancement in a cavity by strong focusing, as shown in figure 5. Similarly to [16], two spherical surfaces with a separation  $L$  form a cavity such that the cavity mode corresponds to a the focused light field configuration in the above discussed strong focusing regime, and is characterized by a focusing parameter  $u$ . We assume that the cavity mode has still a Gaussian transverse envelope, although for a strong focusing regime, the cavity is close to the edge of the stability region.

##### A. Interaction Hamiltonian

With the electrical field operator for an optical mode overlapping with an atom we can easily obtain the coupling strength necessary for a treatment of a two-level atom and the resonant field in a Jaynes–Cummings model. The interaction Hamiltonian of the field with

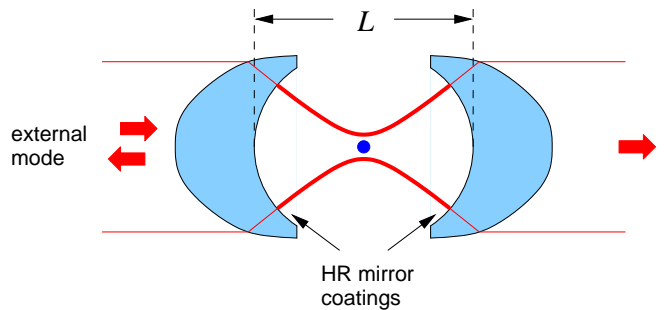


FIG. 5: Concept of an atom in a cavity with a strongly focused resonator mode and a cavity length  $L$ , coupling to collimated running modes with a pair of anaclastic lenses.

an atomic electric dipole moment  $\mathbf{d}$  is given by

$$\begin{aligned} \hat{H}_I &= \hat{\mathbf{E}}_A \cdot \hat{\mathbf{d}} \\ &= i\mathcal{E}d_{\text{eff}}(|e\rangle\langle g|\hat{a}g(\mathbf{x}_A) - |g\rangle\langle e|\hat{a}^\dagger g^*(\mathbf{x}_A)) \\ &=: ig_0(|e\rangle\langle g|\hat{a} - |g\rangle\langle e|\hat{a}^\dagger), \end{aligned} \quad (16)$$

where we choose  $g(\mathbf{x}_A) = 1$  at the location of the atom. We used an effective dipole matrix element  $d_{\text{eff}}$ , which, for a field polarization matching the transition between the two levels and a unit Clebsch-Gordan coefficient, is related to the decay time constant  $\tau$  for the atomic transition by

$$d_{\text{eff}} = \sqrt{\frac{3\epsilon_0 h \lambda^3}{8\pi^2 \tau}}. \quad (17)$$

Therein,  $h$  is the Planck constant and  $\lambda$  the vacuum wavelength corresponding to the optical transition between ground- and excited state [23]. Usually, the coupling strength  $g_0 = \mathcal{E}d_{\text{eff}}$  is quoted to characterize an atom+cavity system, which for a standing wave cavity is given by

$$g_0 = \hbar \sqrt{\frac{\pi c R_{sc}(u)}{\tau L}}. \quad (18)$$

For the D2 transition in a  $^{87}\text{Rb}$  atom with a natural lifetime of  $\tau = 26.25$  ns and a cavity length of  $L = 10$  mm, the expected coupling constant  $g_0$  is shown in figure 6 as a function of the focusing parameter  $u$ . One can see that even for moderate focusing parameters, very large values for the coupling constant can be expected.

##### B. Combining lenses and cavity

A possible geometry with single meniscus elements for an atom–light interface using both field enhancement by a cavity and strong focusing is shown in figure 5. The concave surfaces form the cavity, which is almost concentric - and thus possibly difficult to align. We like to point out that for using our derivation of the focused

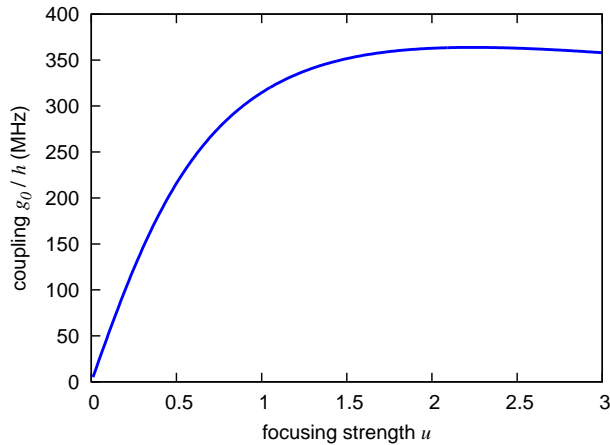


FIG. 6: Coupling parameter  $g_0$  as defined in the Jaynes-Cummings-Hamiltonian in eq. (16) for a two-level transition in  $^{87}\text{Rb}$  as a function of the focusing parameter  $u$ . Even for moderate focusing, large coupling constants exceeding the natural line width can be expected.

light fields [19], such cavity modes require that the mirror surfaces be strictly spherical with a curvature radius  $r_c$ , and  $L \lesssim 2r_c$ . We approximated the focal position for the focused mode as coinciding with the center of the wave front for the focusing calculations, but this does not imply that such a cavity would be concentric.

Practical issues aside, it has been known for a while that the transformation of the cavity mode onto a collimated Gaussian beam can be performed without any error [24, 25]. For a focal length  $f$ , it can be shown that the shape of the convex surface of this anastigmatic lens is an ellipse with half axes  $fn/(n+1)$  in longitudinal, and  $f\sqrt{(n-1)/(n+1)}$  in transverse direction for a fixed refractive index  $n$  of the lens.

Practically, it seems that a half-opening angle for the cavity mode of about  $\Theta_0 \lesssim 45^\circ$  can be achieved, limiting the focusing strength to about  $u_0 = \tan \Theta_0 \lesssim 1$ . Diffrac-

tion at the edges of this resonator will limit the achievable finesse [26]. Under the assumption that the cavity eigenmode still has a Gaussian angular profile, the round-trip diffraction loss  $\epsilon$  at the edges of the resonator for a mode with focusing strength  $u$  for such a cavity can be roughly estimated by

$$\epsilon \approx e^{-2u_0^2/u^2}. \quad (19)$$

For a focusing parameter  $u \approx 0.5$  and  $u_0 \approx 1$ , this loss is on the order of  $10^{-3}$ . With this, a cavity finesse around 100 seems achievable, and the strong coupling regime would be reachable with comparatively large cavity geometries.

## V. CONCLUSION

We have observed the back reflection of a coherent light field from a single atom in near resonance with the light field, and could show that within the limited localization of the atom in our experiment, we understand this in a semiclassical picture for strongly focused light fields presented earlier [19]. We also presented a method of quantizing the fields in such a strongly focused geometry. We find that, when using this geometry in a cavity configuration with its discrete mode spectrum, a coupling constant of an atom with this field much larger than the spontaneous decay time of an atom can be obtained, even for cavities with a relatively large mirror separation. This may imply a technical simplification of atom-photon interfaces to a point that quantum information processing devices based on such interfaces [9, 27] may become much more realistic.

## Acknowledgements

This work is supported by the National Research Foundation & Ministry of Education, Singapore.

- 
- [1] H. J. Kimble, *Physica Scripta* **T76**, 127 (1998).
  - [2] J. Ye, D. W. Vernooy, and H. J. Kimble, *Phys. Rev. Lett.* **83**, 4987 (1999).
  - [3] H. Mabuchi and A. C. Doherty, *Science* **298**, 1372 (2002).
  - [4] D. K. Armani, T. J. Kippenberg, S. M. Spillane, and K. J. Vahala, *Nature* **421**, 925 (2003).
  - [5] M. Hennrich, A. Kuhn, and G. Rempe, *Phys. Rev. Lett.* **94**, 053604 (2005).
  - [6] C. J. Hood, H. J. Kimble, and J. Ye, *Phys. Rev. A* **64**, 033804 (2001).
  - [7] T. Aoki, B. Dayan, E. Wilcut, W. P. Bowen, A. S. Parkins, T. J. Kippenberg, K. J. Vahala, and H. J. Kimble, *Nature* **443**, 671 (2006).
  - [8] T. Steinmetz, Y. Colombe, D. Hunger, T. W. Hänsch, A. Balocchi, R. J. Warburton, and J. Reichel, *Appl. Phys. Lett.* **89**, 111110 (2006).
  - [9] J. I. Cirac, P. Zoller, H. J. Kimble, and H. Mabuchi, *Phys. Rev. Lett.* **78**, 3221 (1997).
  - [10] I. G. I, G. Wrigge, P. Bushev, G. Zumofen, M. Agio, R. Pfab, and V. Sandoghdar, *Phys. Rev. Lett.* **98**, 033601 (2007).
  - [11] G. Wrigge, I. Gerhardt, J. Hwang, G. Zumofen, and V. Sandoghdar, *Nature Physics* **4**, 60 (2008).
  - [12] N. Vamivakas, M. Atature, J. Dreiser, S. T. Yilmaz, A. Badolato, A. K. Swan, B. B. Goldberg, A. Imamoglu, and M. S. Unlu, *Nano Lett.* **7**, 2892 (2007).
  - [13] M. K. Tey, Z. Chen, S. A. Aljunid, B. Chng, F. Huber, G. Maslennikov, and C. Kurtsiefer, *Nature Physics* **4**, 924 (2008), URL [arXiv:0802.3005](https://arxiv.org/abs/0802.3005).
  - [14] S. A. Aljunid, M. K. Tey, B. Chng, T. Liew, G. Maslennikov, V. Scarani, and C. Kurtsiefer, *Phys. Rev. Lett.* **103**, 153601 (2009).

- [15] M. Sondermann, R. Maiwald, H. Konermann, N. Lindlein, U. Peschel, and G. Leuchs, *Appl. Phys. B* **89**, 489 (2007).
- [16] S. E. Morrin, C. C. Yu, and T. W. Mossberg, *Phys. Rev. Lett.* **73**, 1489 (1994).
- [17] A. Haase, B. Hessmo, and J. Schmiedmayer, *Opt. Lett.* **31**, 268 (2006).
- [18] G. Zumofen, N. M. Mojarad, V. Sandoghdar, and M. Agio, *Phys. Rev. Lett.* **101**, 180404 (2008).
- [19] M. K. Tey, S. A. Aljunid, F. Huber, B. Chng, Z. Chen, G. Maslennikov, and C. Kurtsiefer, *New Journal of Physics* **11**, 043011 (2009).
- [20] C. Teo, J. Lee, et al. (2010), in preparation.
- [21] P. Meystre and M. Sargent III, *Elements of Quantum Optics (3rd ed.)* (Springer Verlag, Berlin, 1999).
- [22] M. Stobińska, G. Alber, and G. Leuchs, *Europhys. Lett.* **86**, 14007 (2009), URL <http://arxiv.org/abs/0808.1666v2>.
- [23] C. Cohen-Tannoudji, J. Dupont-Roc, and G. Grynberg, *Photons and Atoms: Introduction into quantum electrodynamics* (Wiley Interscience, New York, 1998).
- [24] I. Sahl, *On burning mirrors and lenses* (Publisher unknown, Baghdad, 984), (See also next reference).
- [25] R. Rashed, *Isis* **81**, 464 (1990).
- [26] A. G. Fox and T. Li, *Proc. IEEE* **51**, 80 (1964).
- [27] J. I. Cirac and P. Zoller, *Physics Today* **57**, 38 (2004).